

Evolution of the acoustic startle response of Mexican cavefish

Alexandra Paz¹, Brittnee McDole¹, Johanna E. Kowalko², Erik R. Duboue², and Alex C. Keene^{1*}

1. Department of Biological Science, Florida Atlantic University, Jupiter, FL 33458
2. Harriet L. Wilkes Honors College, Jupiter, FL 33458

*Address correspondence to:

5353 Parkside Drive
Jupiter, FL 33458

KeeneA@FAU.edu

20 **Abstract**

21 The ability to detect threatening sensory stimuli and initiate an escape response is essential for
22 survival and under stringent evolutionary pressure. In diverse fish species, acoustic stimuli
23 activate Mauthner neurons, which initiate a stereotypical C-start escape response. This reflexive
24 behavior is highly conserved across aquatic species and provides a model for investigating the
25 neural mechanism underlying the evolution of escape behavior. Here, we define evolved
26 differences in the C-start response between populations of the Mexican cavefish, *Astyanax*
27 *mexicanus*. Cave populations of *A. mexicanus* inhabit in an environment devoid of light and
28 macroscopic predation, resulting in evolved differences in diverse morphological and behavioral
29 traits. We find that the C-start is present in multiple populations of cavefish and river-dwelling
30 surface fish, but response kinematics and probability differ between populations. The Pachón
31 population of cavefish have an increased response probability, a slower response and reduction
32 of the maximum bend angle, revealing evolved differences between surface and cave
33 populations. In two other independently evolved populations of cavefish, the response probability
34 and the kinematics of the response differ from one another, as well as from surface fish,
35 suggesting the independent evolution of differences in the C-start response. Investigation of
36 surface-cave hybrids reveals a relationship between angular speed and peak angle, suggesting
37 these two kinematic characteristics are related at the genetic or functional levels. Together, these
38 findings provide support for the use of *A. mexicanus* as a model to investigate the evolution of
39 escape behavior.

40 **Introduction**

41 Predator evasion is essential for survival and is thought to be a critical trait contributing to
42 behavioral adaptation in novel environments (Domenici, 2010). Multiple sensory systems are
43 used to detect predators including olfaction, vision, and mechanotransduction, which all result in
44 the activation of arousal systems (Ferrari et al, 2010; Bleicher et al, 2018; Temizer et al, 2015;
45 Franceschi et al, 2016; Mooney et al, 2016; Suzuki, 2018). The escape responses of a variety of
46 larval fish systems have been studied in detail, including zebrafish, medaka, killifish, and goldfish
47 (Burgess & Granato, 2007; Featherstone, 1991; Canfield, 2006; Fleuren et al, 2018). All of these
48 species exhibit a conserved, highly stereotypical C-start response. The startle response of fish is
49 termed the C-start because of the characteristic c-shaped curve formed by the body during the
50 first stage of the response, which is followed by a smaller counter-bend and rapid swimming
51 (Kalueff et al, 2013). It is also highly stereotyped and plastic, providing a system to examine innate
52 behaviors and their experience-dependent modification (Lopez-Scheir, 2016).

53

54 The escape responses of larval fish are initiated by multiple pairs of highly conserved
55 reticulospinal neurons that receive input from a variety of sensory systems and project to spinal
56 interneurons and motor neurons that innervate the muscles of the trunk (Liu & Fetcho, 1999;
57 Gahtan et al, 2002; Kohashi & Oda, 2008; Bosch & Paul, 1993). Activation of one of these pairs
58 of neurons, the Mauthner cells, initiate a stereotype short latency C-start escape reflex (Burgess
59 & Granato, 2007; Liu & Fetcho, 1999). Mauthner cells receive input from multiple sensory
60 modalities including from the visual, olfactory, and mechanosensory systems (Medan et al, 2018;
61 Kohashi & Oda, 2008; Canfield, 2006; Kimmel et al, 1990; Bhattacharyya et al, 2017). Thus, these
62 neurons receive sensory information and initiate escape reflexes, providing a model for
63 investigating sensory-motor integration (Bierman et al, 2009). Despite its fundamental importance
64 to behavioral evolution, surprisingly little is known about the neural mechanisms through which
65 ecological perturbation shapes the evolution of this escape response.

66

67 The Mexican cavefish, *Astyanax mexicanus* is a powerful model for studying behavioral evolution
68 (Keene, McGaugh, & Yoshizawa, 2015; Gross, 2012). These fish exist as surface fish that inhabit
69 rivers in Mexico and Southern Texas and at least 29 geographically isolated cave-dwelling
70 populations of the same species (Mitchell, Russell, & Elliott, 1977; Jeffery, 2009). The ecology of
71 caves differs dramatically from the surface habitat resulting in the emergence of distinct
72 morphological and behavioral phenotypes. For example, the absence of light in caves is thought
73 to contribute to the evolution of albinism, eye-loss, and circadian rhythm (Keene et al, 2015). As
74 a consequence of these environmentally driven changes, these fish are useful models for
75 investigating convergent trait evolution, and more recently, the evolution of neural circuits
76 mediating behavior (Jaggard et al, 2018; Alie, 2018; Duboué, 2012). Interestingly, no macroscopic
77 predator the caves lack macroscopic predators of *A. mexicanus*, raising the possibility that a lack
78 of selective pressure for predator avoidance contributes to morphological and behavioral
79 evolution in cavefish populations (Pitcher, 1986).

80

81 Prominent changes in sensory processing contribute to behavioral evolution in cavefish. This
82 includes enhanced sensitivity of the lateral line that contributes to prey capture and sleep loss in
83 cavefish (Yoshizawa et al, 2012; Lloyd et al, 2018; Jaggard et al, 2017). Cavefish have also
84 evolved increased sensitivity to tastants and odorants, presumably to support efficient foraging
85 in the absence of visual cues (Shiriagin & Korschning, 2019; Bibliowicz, 2013; Hinaux et al, 2016).
86 Additionally, *A. mexicanus* use acoustic stimulation to communicate, and a recent report
87 highlights the differences in this communication between surface and cave morphs (Hyacinthe et
88 al, 2019). The diversity of evolved changes in sensory processing combined with the robust
89 ecological differences raises the possibility that the startle reflex may differ between populations
90 of *A. mexicanus*.

91

92 Here, we systematically investigate the evolution of the C-start response to acoustic stimuli in
93 multiple *A. mexicanus* population. We find differences in both response probability and kinematics
94 between surface fish larvae and three different populations of cavefish. These findings support
95 the notion that the ecological differences between cave and river environments contribute to
96 differences in escape behavior and provide a platform for investigating the evolution of neural
97 circuits contributing to sensory-motor integration.

98 **Results**

99 To quantify differences in startle response, we constructed a system to produce acoustic pulses
100 similar to those shown to induce startle behavior in zebrafish (Burgess & Granato, 2007;
101 Bhandiwad, 2013; Zeddies & Fay, 2005). Fish were individually placed in custom-designed wells
102 attached to a vibration exciter that provided acoustic stimuli. Behavior of the fish was recorded
103 throughout the stimulation using a high-speed camera (Fig 1A). We first compared the probability
104 of 6 day post fertilization (dpf) surface fish and Pachón cavefish initiating a C-start in response to
105 acoustic stimulation. We found that both surface and Pachón cave populations responded to
106 acoustic stimuli with a stereotyped response consisting of simultaneous head and tail turning, as
107 observed during classic C-start escape reflexes that have been characterized in zebrafish and
108 other aquatic models (Burgess & Granato, 2007; Featherstone, 1991; Canfield, 2006; Fleuren et
109 al, 2018). To determine whether the sensitivity required to elicit an escape response differed
110 between populations, we quantified the probability of C-start initiation in surface fish and Pachón
111 cavefish at multiple vibration intensities and found that cavefish exhibit an increased response
112 probability to vibrations at 31 dB (surface fish 67%, cavefish: 53%) and 35 dB (surface fish 74%,
113 cavefish: 90%), but not 28 dB (surface fish: 47%, cavefish: 43%) (Fig 1B). These data
114 demonstrate that Pachón cavefish have a more acute sensitivity to vibrations relative to their
115 surface conspecifics.

116

117 In order to compare C-start kinematics between surface fish and cavefish, we quantified response
118 latency, maximum change in orientation (referred to as “peak bend angle”), and angular speed,
119 and found that the responses of surface fish and Pachón cavefish differ in all quantified kinematic
120 parameters (Fig 2A & B). The C-start responses of Pachón cavefish are characterized by a
121 decrease in angular speed and peak bend angle compared to surface fish, with Pachón turning
122 approximately 3°/ms more slowly and to a peak bend angle that is smaller in magnitude by almost
123 20° relative to surface fish (Fig 2C & D). Pachón larvae also displayed significantly longer

124 response latencies than surface fish larvae (Fig 2E). In surface fish, the shortest latency C-starts
125 were initiated 7-9 ms after stimulus onset, in contrast to Pachón larvae in which the shortest
126 latency C-starts were initiated 11-13 ms after stimulus onset (Fig 2F). Together these data
127 suggest that cavefish have developed substantial differences in the C-start response.

128

129 In teleosts, Mauthner neurons integrate visual stimuli, and a loom stimulus is enough to initiate a
130 C-start response (Temizer et al, 2015; Bhattacharyya et al, 2017). Cavefish can detect light and
131 sense looming stimuli, despite eye degeneration, raising the possibility that light modulates the
132 C-start response (Yoshizawa & Jeffery, 2008). To assess the influence of visual input on response
133 probability and kinematics we assayed escape response under light and dark conditions. The
134 presence of light had no effect on response probability, response latency, or angular speed in
135 cavefish or surface fish (Fig 3A-C). In goldfish, it was found that peak C-start bend angle was
136 predictable based off of a fish's orientation relative to the startle-inducing stimulus, except for
137 situations where the predicted trajectory was blocked by a wall (Eaton & Emberley, 1991). This
138 trend was true even when C-starts were initiated from rest, precluding the possibility that the
139 lateral line was influencing escape kinematics. Furthermore, in zebrafish it has been shown that
140 peak bend angle is a reliable predictor of escape trajectory (Bhattacharyya et al, 2017). In dark
141 conditions, surface fish display an increase in peak bend angle , while no difference is detected
142 in cavefish (Fig 3D). These data suggest that, as with goldfish, the escape path of surface fish is
143 visually informed.

144 Independently evolved populations of cavefish have converged on numerous behavioral and
145 morphological traits (Keene, McGaugh, & Yoshizawa, 2015; Gross, 2012), providing a powerful
146 system for examining whether convergent traits arise through similar or distinct genetic
147 mechanisms. To determine whether the changes in C-start probability and kinematics are shared
148 across cavefish populations, we measured response in Molino and Tinaja cavefish. While Tinaja

149 larvae exhibit a response probability similar to that of surface fish, larvae from the Molino
150 population exhibited a 98% response probability, which was significantly higher than surface fish
151 and any of the cavefish populations (Fig 4A). Unlike Pachón larvae, Molino and Tinaja did not
152 exhibit any differences in response latency relative to surface fish (Fig 4B). However, angular
153 speed was reduced in both Tinaja and Molino populations (Fig 4C) while the peak bend angle
154 was significantly reduced in Tinaja compared to surface fish (Fig 4D). Together, these findings
155 reveal convergence on a decrease in angular speed during the C-start response in cavefish. On
156 the other hand, the variety in latency, peak bend angle, and response probability observed in the
157 three cavefish populations analyzed here reveal the evolution of unique kinematic changes across
158 all three cavefish populations.

159
160 It is possible that independent genetic mechanisms contribute to different kinematic components
161 of the C-start, or that they have evolved through shared genetic architecture. A benefit of *A.*
162 *mexicanus* is that cavefish and surface fish populations are interfertile, producing hybrid offspring
163 that possess behavioral and morphological characteristics ranging from cave-like to surface-like,
164 as well as intermediate phenotypes. To differentiate between these possibilities, we quantified
165 the kinematics of C-start responses of surface-cave F₂ hybrid fish. The response probability of
166 F₂ hybrid fish was intermediate to pure surface and Pachón fish, but this did not reach significance
167 (Fig 5A). Significant differences in latency were not detected between hybrid fish and surface or
168 Pachón populations, with the range of values exhibited by F₂ hybrids encompassing the full range
169 of values seen in surface and Pachón fish. Though no significant differences were identified in
170 these data, it is worth noting that the mean value for the F₂ hybrids (16 ms) matched that of
171 Pachón cavefish (16 ms), but not that of surface fish (14 ms) (Fig 5B). Similarly, the peak bend
172 angle of F₂ hybrids resembled those of Pachón cave fish, differing significantly from the larger
173 bend seen in surface fish responses (Fig 5C). The angular speed of F₂ hybrids was intermediate
174 to that of surface and Pachón fish (Fig 5D). To determine the relationship between components

175 of the C-start response, we quantified the correlation between each pair of kinematic parameters.
176 No correlation was observed between response latency and peak angle or angular speed,
177 however there was a significant correlation between angular velocity and peak angle. Taken
178 together, these findings suggest that there are a variety of factors influencing the various
179 kinematic parameters that compose the C-start response.

180

181

182 **Discussion**

183 The C-start response represents a primary mechanism for predator avoidance in fish and
184 amphibians (Yasugi & Hori, 2012; Walker et al, 2005; Fuiman, 1993) Here, we identify evolved
185 changes in the C-start response in multiple independent populations of *A. mexicanus*. There are
186 many differences between the ecology of caves and that of rivers and lakes inhabited by surface
187 fish including changes in food availability, changes in water quality, loss of circadian cues, and
188 reduced predation (Keene et al, 2015). It is possible that, since there is a near absence of
189 predators in the caves, the changes observed in cavefish are due to relaxed interspecies selective
190 pressure in the cave environments. However, adult surface and cave populations of *A. mexicanus*
191 consume their larvae, raising the possibility that the C-start remains critical for intra-species
192 predation. Further investigation of the ecology of early life environment within the natural setting
193 may inform the cause of the evolved changes in the C-start.

194

195 In fish, escape responses can be characterized into those which occur quickly (short latency C-
196 starts) and those that emerge later (long latency C-starts) (Burgess & Granato, 2007). Ablation of
197 the Mauthner neurons completely abolishes short latency C-starts in goldfish and zebrafish, but
198 not longer latency C-starts, which are initiated by a different set of reticulospinal neurons (Kohashi
199 & Oda, 2008; Burgess & Granato, 2007; Eaton et al, 1982; Liu & Fetcho, 1999). We observed
200 that the latency is significantly greater in Pachón cavefish than in surface fish, raising the
201 possibility that differences in Mauthner neuron signaling may contribute to the observed
202 differences in startle kinematics. In zebrafish, the frequency distribution of C-start initiation latency
203 values produces a bimodal curve, with separate peaks representing short latency C-starts and
204 less frequent long latency C-starts (Burgess & Granato, 2007; Takahashi et al, 2017; Issa et al,
205 2011). In our frequency analysis we did not identify separate peaks, however this is likely due to
206 sample size, not a lack of long latency responses. Future studies testing a greater number of

207 individuals may provide insight into how the reticulospinal escape network has evolved and the
208 intrapopulation variation in this response.

209 We identified an increased probability of eliciting a startle response in Pachón and Molino larvae.
210 It is possible that this is due to altered sensory detection of the acoustic stimuli, or due to changes
211 at the level of processing that affect the threshold of Mauthner neuron activation. Adult surface
212 and cavefish respond to click-like sounds that signal aggression, revealing the presence of
213 acoustic communication between conspecifics in this species (Hyacinthe et al, 2019). Previous
214 analysis of auditory sensitivity in *Astyanax* did not identify differences between surface and cave
215 populations, supporting the notion that the differences observed are at the level of sensory
216 processing, rather than detection (Popper, 1970, Hinaux, 2016). Therefore, it is unlikely that
217 differences in sensory detection underlie the enhanced response probability in cavefish.

218 The kinematics of the C-start response differed between all three cavefish populations and
219 surface fish. In Pachón and Tinaja cavefish, this is marked by a reduced peak angle within the
220 C-start response. Further, the differences in kinematic changes across all three cave populations,
221 raise the possibility that different genetic and neural mechanism underlie changes in this escape
222 response across different population.

223

224 Identifying the behavioral and neuronal components of the C-Start response that are associated
225 with effective interspecies and intraspecies escape may provide insight into the ecological factors
226 contributing to the evolution of the C-start. In guppies, increased angular speed during the first
227 phase of fast start escapes has been correlated with more effective predator evasion, raising the
228 possibility that individual kinematic parameters contribute to successful predator avoidance
229 (Walker et al, 2005). Interestingly, all cave population analyzed here exhibit decreased angular
230 speed. Further, it is extremely likely that a quick latency increases the likelihood of successful
231 evasion. While it may seem intuitive to predict that an increase in response probability would be

232 beneficial in successfully avoiding predators, in a situation where predators are known to rely
233 heavily on mechanosensory stimuli for prey capture, such as in cavefish, initiation of a startle
234 response could potentially be detrimental (Lloyd et al, 2018; Yoshizawa et al, 2010). These data
235 suggest that the C-start responses of cavefish may be less effective for successful predator
236 evasion as a result of the relaxation of predation in the cave environment.

237

238 The escape response is likely to be energetically expensive, and therefore extremely detrimental
239 in the nutrient-limited cave environment. A possible explanation for the increased response
240 probability of Pachón larvae to vibrational stimuli may be related to a shift in feeding strategy. In
241 hunting archer fish and goldfish, C-shaped flexions have been associated with prey capture (Wohl
242 & Schuster, 2007; Canfield 2007). Furthermore, in goldfish, this feeding behavior has been
243 correlated with firing of the Mauthner neurons (Canfield & Rose, 1993). In cave populations of
244 *Astyanax*, loss of eyesight has resulted in a shift in prey capture behavior involving the use of the
245 lateral line to sense prey, which are captured using a C-bend, similar to the C-start behavior we
246 examine here. This is in contrast to sight-dependent prey capture observed in surface fish which
247 consists of J-shaped turns and a of a head-on approach. Interestingly, Pachón cavefish were able
248 to successfully capture prey even after complete pharmaceutical ablation of the lateral line, but
249 were unable to capture dead prey, suggesting hat alternate modes of perception of movement
250 are being utilized (Lloyd et al, 2018). Taken together, these data suggest that the increase in
251 acoustically driven C-start responses observed in cavefish may be driven by a shift in feeding
252 strategy.

253

254 Powerful genetic approaches in zebrafish have provided extensive mechanistic insight into the
255 function of the Mauthner neurons (Burgess et al, 2014; Shimazaki et al, 2019; Stil & Drapeau,
256 2015; Monesson-Olson et al, 2014). This includes the use of genetically expressed Ca²⁺ sensors
257 to identify how the activity of these neurons is modulated and the use of GAL4-based genetic

258 screens to identify additional circuits that regulate the startle response (Takahashi et al, 2017;
259 Lacoste et al, 2015; Choe et al, 2013). Recently, many of these technologies including GCaMP
260 imaging, *tol2* transgenesis, and CRISPR gene editing have been developed in *A. mexicanus*
261 (Stahl et al, 2019; Kowalko et al, 2018; Elipot et al, 2014). The application of these genetic
262 approaches has potential to define functional differences between surface fish and cavefish and
263 provide mechanistic insight into evolved differences between the populations. For example, the
264 anatomy and activity of Mauthner neurons can be directly compared between individual
265 populations. Our identification of differences in response probability and kinematics between *A.*
266 *mexicanus* populations position this system as a powerful model for examining the evolution of
267 the escape responses and sensory-motor integration.

268 **Methods**

269 Animal husbandry was carried out as previously described (Borowsky, 2008; Stahl et al, 2019)
270 and all protocols were approved by the IACUC Florida Atlantic University (Protocols A15-32 and
271 A16-04). Fish were housed in the Florida Atlantic University core facilities at $23 \pm 1^\circ\text{C}$ constant
272 water temperature throughout rearing for behavior experiments (Borowsky, 2008). Lights were
273 kept on a 14:10 hr light-dark cycle that remained constant throughout the animal's lifetime. Light
274 intensity was kept between 25–40. Larvae were raised in 200ml bowls.

275

276 **Behavioral experiments**

277 C-start responses were elicited according to methods previously utilized for zebrafish (Burgess &
278 Granato, 2007; Bhandiwad et al, 2013; Zeddis & Fay, 2005). All behavioral testing was done
279 between ZT5 and ZT9 (Zeitgeber time) in a temperature controlled room maintained between 23
280 and 25°C. For all assays individual 6 dpf larvae were placed within 15x15x9 cm square wells on
281 a custom 3D-printed polyactic acid plate (Autodesk Fusion 360; San Rafael, CA; Creality CR10
282 Max; Guangdong, China) and allowed to acclimate for 10 minutes before being exposed to a
283 single stimulus. The plates were securely screwed onto a vertically oriented vibration exciter
284 (Type 4810; Brüel and Kjaer, Duluth, GA) controlled by a multifunction I/O device (PCIe-6321;
285 National Instruments, Austin, TX). Stimuli were 500 Hz square waves of 50 ms duration generated
286 using Labview 2018 v.18.0f2 (National Instruments, Austin, TX) and were of an intensity of 31 dB,
287 unless otherwise stated. Stimulus intensity was determined using a Check Mate CM-130 SPL
288 meter (Galaxy Audio; Wichita, KS) held approximately 2 cm above the center of the vibrating
289 apparatus. Plates had between 1 and 18 wells. For trials conducted on plates with greater than 6
290 wells, recording was done from above with the well placed directly over the center of the exciter
291 to avoid shifting the center of mass away from the source of the stimulus. In these cases, lighting
292 was provided from below using LED strips in addition to overhead ceiling lights. For trials

293 conducted using plates with 6 wells or fewer, recording was done from below and illumination was
294 done from above using LED strips and a polycarbonate sheet for diffusing light. Infrared light strips
295 (940 nm) were used for all light/dark experiments. For trials conducted for the light condition, white
296 light LED strips were also used.

297 Video was acquired at 1000 frames per second using an FPS 2000 high speed camera (The Slow
298 Motion Camera Company Limited; London, UK).

299

300

301 **Analysis of C-start responses**

302 C-start responses were identified as accelerated, simultaneous flexion of the head and tail in the
303 same direction. Response probability is reported as the total proportion of larvae that exhibited a
304 C-start response. Kinematic analysis was performed by separately analyzing various parameters
305 of the C-start response as previously done in zebrafish (Issa et al, 2011; Burgess & Granato,
306 2007; Takahashi et al, 2017). The “angle” tool available on ImageJ 1.52a (National Institutes of
307 Health; Bethesda, MD) was used to determine the orientation of the larvae by measuring the
308 angle formed by a horizontal line and a line drawn along the midline of the fish from the anterior-
309 most point of the swim bladder to the anterior-most point on the head. Measurements were
310 subsequently standardized to the orientation of the larva 1 ms before stimulus onset.

311 Response latency was defined as the time between stimulus onset and a change in orientation of
312 10°. Peak angle was identified as the maximum change in orientation before a change in direction
313 back toward the original orientation. Speed was determined as the slope of the best-fit line for
314 change in body orientation from the point in time designated as the latency to the time of the peak
315 angle.

316

317

318

319 **Statistical Analysis**

320 All statistical tests were conducted on GraphPad Prism 8.2.1 or RStudio 1.2.1335. Differences in
321 response probability were analyzed using Fisher's Exact Test, except for analyses of 2x3 tables,
322 which were analyzed using a χ^2 test. All error bars on response probability data denote margin of
323 error of the sample proportion calculated using a z^* -value of 1.96. Post-hoc analysis was
324 conducted on results that indicated a significant difference ($\alpha \leq 0.05$) via pairwise χ^2 tests and
325 Bonferroni correction of p-values. Normality of kinematic data was assessed using a Shapiro-Wilk
326 test. Data that did not pass the normality test were subsequently assessed using the Mann-
327 Whitney test and data that did pass the normality test were assessed using an unpaired t-test. In
328 cases involving more than 2 populations, a one-way ANOVA was used followed by Tukey's test
329 in cases that the results of the ANOVA indicated significant differences ($\alpha \leq 0.05$). Correlation
330 between kinematic parameters was assessed using Spearman's rank order correlation.

331

332 **References**

333 Ali, D. W., Drapeau, P., & Legendre, P. (2000). Development of spontaneous glycinergic
334 currents in the Mauthner neuron of the zebrafish embryo. *Journal of Neurophysiology*,
335 84(4), 1726–1736. <https://doi.org/10.1152/jn.2000.84.4.1726>

336 Alié, A., Devos, L., Torres-Paz, J., Prunier, L., Boulet, F., Blin, M., ... Retaux, S. (2018).
337 Developmental evolution of the forebrain in cavefish, from natural variations in
338 neuropeptides to behavior. *eLife*, 7. <https://doi.org/10.7554/eLife.32808>

339 Alié, A., Devos, L., Torres-Paz, J., Prunier, L., Boulet, F., Blin, M., ... Retaux, S. (2018).
340 Developmental evolution of the forebrain in cavefish, from natural variations in
341 neuropeptides to behavior. *eLife*, 7. <https://doi.org/10.7554/eLife.32808>

342 Bhandiwad, A. A., Zeddies, D. G., Raible, D. W., Rubel, E. W., & Sisneros, J. A. (2013).
343 Auditory sensitivity of larval zebrafish (*Danio rerio*) measured using a behavioral prepulse
344 inhibition assay. *Journal of Experimental Biology*, 216(18), 3504–3513.
345 <https://doi.org/10.1242/jeb.087635>

346 Bhattacharyya, K., McLean, D. L., & MacIver, M. A. (2017). Visual Threat Assessment and
347 Reticulospinal Encoding of Calibrated Responses in Larval Zebrafish. *Current Biology* :
348 *CB*, 27(18), 2751-2762.e6. <https://doi.org/10.1016/j.cub.2017.08.012>

349 Bibliowicz, J., Alié, A., Espinasa, L., Yoshizawa, M., Blin, M., Hinaux, H., ... Rétaux, S.
350 (2013). Differences in chemosensory response between eyed and eyeless *Astyanax*
351 *mexicanus* of the Rio Subterráneo cave. *EvoDevo*, 4(1), 25. <https://doi.org/10.1186/2041-9139-4-25>

353 Bierman, H. S., Zottoli, S. J., & Hale, M. E. (2009). Evolution of the mauthner axon cap. *Brain,*
354 *Behavior and Evolution*, 73(3), 174–187. <https://doi.org/10.1159/000222562>

355 Bleicher, S. S., Ylönen, H., Käpälä, T., & Haapakoski, M. (2018). Olfactory cues and the value
356 of information: voles interpret cues based on recent predator encounters. *Behavioral*
357 *Ecology and Sociobiology*, 72(12), 187. <https://doi.org/10.1007/s00265-018-2600-9>

358 Borowsky, R. (2008). Handling *Astyanax mexicanus* Eggs and Fry. *CSH Protocols*, 2008,
359 *pdb.prot5093*. <https://doi.org/10.1101/pdb.prot5093>

360 Bosch, T. J., & Paul, D. H. (1993). Differential responses of single reticulospinal cells to
361 spatially localized stimulation of the optic tectum in a teleost fish, *Salmo trutta*. *The*
362 *European Journal of Neuroscience*, 5(6), 742–750. <https://doi.org/10.1111/j.1460-9568.1993.tb00538.x>

364 Buchan, J. R. (2014). mRNP granules. Assembly, function, and connections with disease. *RNA*
365 *Biology*, 11(8), 1019–1030. <https://doi.org/10.4161/15476286.2014.972208>

366 Bulletin, P. W.-F., & 1981, undefined. (n.d.). TO PREDATION BY A BITING
367 PLANKTIVORE, AMPHIPRION PERCULA. *National Marine Fisheries Service*.

368 Burgess, H. A., & Granato, M. (2007). Sensorimotor gating in larval zebrafish. *Journal of*
369 *Neuroscience*, 27(18), 4984–4994. <https://doi.org/10.1523/JNEUROSCI.0615-07.2007>

370 Canfield, J. G., & Rose, G. J. (1993). Activation of Mauthner neurons during prey capture.
371 *Journal of Comparative Physiology A*, 172(5), 611–618.
372 <https://doi.org/10.1007/BF00213683>

373 Canfield, J. G. (2006). Functional evidence for visuospatial coding in the Mauthner neuron.
374 *Brain, Behavior and Evolution*, 67(4), 188–202. <https://doi.org/10.1159/000091652>

375 Chin, J. S. R., Gassant, C. E., Amaral, P. M., Lloyd, E., Stahl, B. A., Jaggard, J. B., ... Duboue,
376 E. R. (2018). Convergence on reduced stress behavior in the Mexican blind cavefish.
377 *Developmental Biology*, 441(2), 319–327. <https://doi.org/10.1016/j.ydbio.2018.05.009>

378 Choe, S. K., Nakamura, M., Ladam, F., Etheridge, L., & Sagerström, C. G. (2012). A Gal4/UAS
379 system for conditional transgene expression in rhombomere 4 of the zebrafish hindbrain.
380 *Developmental Dynamics*, 241(6), 1125–1132. <https://doi.org/10.1002/dvdy.23794>

381 De Franceschi, G., Vivattanasarn, T., Saleem, A. B., & Solomon, S. G. (2016). Vision Guides
382 Selection of Freeze or Flight Defense Strategies in Mice. *Current Biology : CB*, 26(16),
383 2150–2154. <https://doi.org/10.1016/j.cub.2016.06.006>

384 Domenici, P. (2010). Context-dependent variability in the components of fish escape response:
385 Integrating locomotor performance and behavior. *Journal of Experimental Zoology Part A:*
386 *Ecological Genetics and Physiology*, 313 A(2), 59–79. <https://doi.org/10.1002/jez.580>

387 Dunn, T. W., Gebhardt, C., Naumann, E. A., Riegler, C., Ahrens, M. B., Engert, F., & Del Bene,
388 F. (2016). Neural Circuits Underlying Visually Evoked Escapes in Larval Zebrafish.
389 <https://doi.org/10.1016/j.neuron.2015.12.021>

390 Eaton, R. C., Farley, R. D., Kimmel, C. B., & Schabtach, E. (1977). Functional development in
391 the Mauthner cell system of embryos and larvae of the zebra fish. *Journal of Neurobiology*,
392 8(2), 151–172. <https://doi.org/10.1002/neu.480080207>

393 Eaton, R. C., & Emberley, D. S. (1991). How stimulus direction determines the trajectory of the
394 Mauthner-initiated escape response in a teleost fish. *The Journal of Experimental Biology*,
395 161, 469–487.

396 Eaton, R. C., Lavender, W. A., & Wieland, C. M. (1982). Alternative neural pathways initiate
397 fast-start responses following lesions of the mauthner neuron in goldfish. *Journal of*
398 *Comparative Physiology □ A*, 145(4), 485–496. <https://doi.org/10.1007/BF00612814>

399 Eaton, R. C., & Emberley, D. S. (1991). *HOW STIMULUS DIRECTION DETERMINES THE*
400 *TRAJECTORY OF THE MAUTHNER-INITIATED ESCAPE RESPONSE IN A TELEOST*
401 *FISH* (Vol. 161).

402 Elipot, Y., Legendre, L., Père, S., Sohm, F., & Rétaux, S. (2014). Astyanax transgenesis and
403 husbandry: how cavefish enters the laboratory. *Zebrafish*, 11(4), 291–299.
404 <https://doi.org/10.1089/zeb.2014.1005>

405 Featherstone, D., Drewes, C. D., & Coats, J. R. (1991). *SHORT COMMUNICATION*
406 *NONINVASIVE DETECTION OF ELECTRICAL EVENTS DURING THE STARTLE*
407 *RESPONSE IN LARVAL MEDAKA*. *J. exp. Biol* (Vol. 158).

408 Ferrari, M. C. O., Wisenden, B. D., & Chivers, D. P. (2010). Chemical ecology of predator-prey
409 interactions in aquatic ecosystems: A review and prospectus. *Canadian Journal of Zoology*.
410 <https://doi.org/10.1139/Z10-029>

411 Fetcho, J. R. (1991). Spinal network of the Mauthner cell. *Brain, Behavior and Evolution*, 37(5),
412 298–316. <https://doi.org/10.1159/000114367>

413 Fleuren, M., Van Leeuwen, J. L., Quicazan-Rubio, E. M., Pieters, R. P. M., Pollux, B. J. A., &
414 Voesenek, C. J. (2018). Three-dimensional analysis of the fast-start escape response of the
415 least killifish, *Heterandria formosa*. *Journal of Experimental Biology*, 221(7).
416 <https://doi.org/10.1242/jeb.168609>

417 Fuiman, L. A. (1993). Development of predator evasion in Atlantic herring, *Clupea harengus* L.
418 *Animal Behaviour*, 45(6), 1101–1116. <https://doi.org/10.1006/anbe.1993.1135>

419 Gahtan, E., Sankrithi, N., Campos, J. B., & O’Malley, D. M. (2002). Evidence for a widespread
420 brain stem escape network in larval zebrafish. *Journal of Neurophysiology*, 87(1), 608–614.
421 <https://doi.org/10.1152/jn.00596.2001>

422 Gross, J. B. (2012). The complex origin of Astyanax cavefish. *BMC Evolutionary Biology*.
423 <https://doi.org/10.1186/1471-2148-12-105>

424 Heap, L. A. L., Vanwalleghem, G., Thompson, A. W., Favre-Bulle, I. A., & Scott, E. K. (2018).
425 Luminance Changes Drive Directional Startle through a Thalamic Pathway. *Neuron*, 99(2),
426 293-301.e4. <https://doi.org/10.1016/j.neuron.2018.06.013>

427 Hinaux, H., Devos, L., Blin, M., Elipot, Y., Bibliowicz, J., Alié, A., & Rétaux, S. (2016).
428 Sensory evolution in blind cavefish is driven by early embryonic events during gastrulation
429 and neurulation. *Development (Cambridge, England)*, 143(23), 4521–4532.
430 <https://doi.org/10.1242/dev.141291>

431 Hyacinthe, C., Attia, J., & Rétaux, S. (2019). Evolution of acoustic communication in blind
432 cavefish. *Nature Communications*, 10(1), 4231. <https://doi.org/10.1038/s41467-019-12078-9>

434 Issa, F. A., O'Brien, G., Kettunen, P., Sagasti, A., Glanzman, D. L., & Papazian, D. M. (2011).
435 Neural circuit activity in freely behaving zebrafish (*Danio rerio*). *The Journal of*
436 *Experimental Biology*, 214(Pt 6), 1028–1038. <https://doi.org/10.1242/jeb.048876>

437 Jaggard, J. B., Stahl, B. A., Lloyd, E., Prober, D. A., Duboue, E. R., & Keene, A. C. (2018).
438 Hypocretin underlies the evolution of sleep loss in the Mexican cavefish. *ELife*, 7.
439 <https://doi.org/10.7554/eLife.32637>

440 Jaggard, J., Robinson, B. G., Stahl, B. A., Oh, I., Masek, P., Yoshizawa, M., & Keene, A. C.
441 (2017). The lateral line confers evolutionarily derived sleep loss in the Mexican cavefish.
442 *Journal of Experimental Biology*, 220(2), 284–293. <https://doi.org/10.1242/jeb.145128>

443 Jain, S., Wheeler, J. R., Walters, R. W., Agrawal, A., Barsic, A., & Parker, R. (2016). ATPase-
444 Modulated Stress Granules Contain a Diverse Proteome and Substructure. *Cell*, 164(3),
445 487–498. <https://doi.org/10.1016/j.cell.2015.12.038>

446 Jeffery, W. R. (2009). Regressive evolution in *Astyanax* cavefish. *Annual Review of Genetics*,
447 43, 25–47. <https://doi.org/10.1146/annurev-genet-102108-134216>

448 Kalueff, A. V., Gebhardt, M., Stewart, A. M., Cachat, J. M., Brimmer, M., Chawla, J. S., ...
449 Schneider, H. (2013, March 1). Towards a comprehensive catalog of zebrafish behavior 1.0
450 and beyond. *Zebrafish*. <https://doi.org/10.1089/zeb.2012.0861>

451 Keene, A. C., Yoshizawa, M., & McGaugh, S. E. (2015). *Biology and Evolution of the Mexican*
452 *Cavefish. Biology and Evolution of the Mexican Cavefish*. Elsevier Inc.
453 <https://doi.org/10.1016/C2014-0-01426-8>

454 Kimmel, C. B., Hatta, K., & Metcalfe, W. K. (1990). Early axonal contacts during development
455 of an identified dendrite in the brain of the zebrafish. *Neuron*, 4(4), 535–545.
456 [https://doi.org/10.1016/0896-6273\(90\)90111-r](https://doi.org/10.1016/0896-6273(90)90111-r)

457 Klaassen, H., Wang, Y., Adamski, K., Rohner, N., & Kowalko, J. E. (2018). CRISPR
458 mutagenesis confirms the role of oca2 in melanin pigmentation in *Astyanax mexicanus*.
459 *Developmental Biology*, 441(2), 313–318. <https://doi.org/10.1016/j.ydbio.2018.03.014>

460 Klaassen, H., Wang, Y., Adamski, K., Rohner, N., & Kowalko, J. E. (2018). CRISPR
461 mutagenesis confirms the role of oca2 in melanin pigmentation in *Astyanax mexicanus*.
462 *Developmental Biology*, 441(2), 313–318. <https://doi.org/10.1016/j.ydbio.2018.03.014>

463 Kohashi, T., & Oda, Y. (2008). Behavioral/Systems/Cognitive Initiation of Mauthner-or Non-
464 Mauthner-Mediated Fast Escape Evoked by Different Modes of Sensory Input.
465 <https://doi.org/10.1523/JNEUROSCI.1435-08.2008>

466 Korn, H., & Faber, D. S. (2005, July 7). The Mauthner cell half a century later: A
467 neurobiological model for decision-making? *Neuron*.
468 <https://doi.org/10.1016/j.neuron.2005.05.019>

469 Lacoste, A. M. B., Schoppik, D., Robson, D. N., Haesemeyer, M., Portugues, R., Li, J. M., ...
470 Schier, A. F. (2015). A Convergent and essential interneuron pathway for mauthner-cell-
471 mediated escapes. *Current Biology*, 25(11), 1526–1534.
472 <https://doi.org/10.1016/j.cub.2015.04.025>

473 Liu, K. S., & Fecho, J. R. (1999). Laser ablations reveal functional relationships of segmental
474 hindbrain neurons in zebrafish. *Neuron*, 23(2), 325–335. [https://doi.org/10.1016/S0896-6273\(00\)80783-7](https://doi.org/10.1016/S0896-6273(00)80783-7)

475

476 Liu, K. S., Gray, M., Otto, S. J., Fecho, J. R., & Beattie, C. E. (2003). Mutations in deadly
477 seven/notch1a reveal developmental plasticity in the escape response circuit. *The Journal of
478 Neuroscience : The Official Journal of the Society for Neuroscience*, 23(22), 8159–8166.
479 Retrieved from <http://www.ncbi.nlm.nih.gov/pubmed/12954879>

480 Liu, K. S., Gray, M., Otto, S. J., Fecho, J. R., & Beattie, C. E. (2003). Mutations in deadly
481 seven/notch1a reveal developmental plasticity in the escape response circuit. *The Journal of
482 Neuroscience : The Official Journal of the Society for Neuroscience*, 23(22), 8159–8166.
483 <https://doi.org/10.1523/JNEUROSCI.23-22-08159.2003>

484 Lloyd, E., Olive, C., Stahl, B. A., Jaggard, J. B., Amaral, P., Duboué, E. R., & Keene, A. C.
485 (2018). Evolutionary shift towards lateral line dependent prey capture behavior in the blind
486 Mexican cavefish. *Developmental Biology*, 441(2), 328–337.
487 <https://doi.org/10.1016/j.ydbio.2018.04.027>

488 López-Schier, H. (2019). Neuroplasticity in the acoustic startle reflex in larval zebrafish. *Current
489 Opinion in Neurobiology*, 54, 134–139. <https://doi.org/10.1016/j.conb.2018.10.004>

490 Medan, V., Mäki-Marttunen, T., Sztarker, J., & Preuss, T. (2018). Differential processing in
491 modality-specific Mauthner cell dendrites. *Journal of Physiology*, 596(4), 667–689.
492 <https://doi.org/10.1113/JP274861>

493 Medan, V., & Preuss, T. (2014). The Mauthner-cell circuit of fish as a model system for startle
494 plasticity. *Journal of Physiology Paris*. <https://doi.org/10.1016/j.jphysparis.2014.07.006>

495 Miller, T. H., Clements, K., Ahn, S., Park, X. C., Eoon, X., Ji, H., ... Issa, A. (2017).
496 Systems/Circuits Social Status-Dependent Shift in Neural Circuit Activation Affects
497 Decision Making. <https://doi.org/10.1523/JNEUROSCI.1548-16.2017>

498 Mitchell, R. W. & Russell, W. H. & Elliott, William. (1977). Mexican eyeless characin fishes,
499 genus *Astyanax*: Environment, distribution, and evolution. Spec. Publ. Mus. Texas Tech.
500 Univ.. 12. 1-89.

501 Monesson-Olson, B. D., Browning-Kamins, J., Aziz-Bose, R., Kreines, F., & Trapani, J. G.
502 (2014). Optical stimulation of zebrafish hair cells expressing channelrhodopsin-2. *PLoS
503 One*, 9(5), e96641. <https://doi.org/10.1371/journal.pone.0096641>

504 Mooney, T. A., Samson, J. E., Schlunk, A. D., & Zacarias, S. (2016). Loudness-dependent
505 behavioral responses and habituation to sound by the longfin squid (*Doryteuthis pealeii*).
506 *Journal of Comparative Physiology. A, Neuroethology, Sensory, Neural, and Behavioral*
507 *Physiology*, 202(7), 489–501. <https://doi.org/10.1007/s00359-016-1092-1>

508 Nissanov, J., Eaton, R. C., & DiDomenico, R. (1990). The motor output of the Mauthner cell, a
509 reticulospinal command neuron. *Brain Research*, 517(1–2), 88–98.
510 [https://doi.org/10.1016/0006-8993\(90\)91012-6](https://doi.org/10.1016/0006-8993(90)91012-6)

511 Paz, A. M., & Zhang, X.-N. (2018). The GMO Industry: A Neglected Earthly Frontier. *Journal*
512 *of Hunger and Environmental Nutrition*, 13(2).
513 <https://doi.org/10.1080/19320248.2016.1227755>

514 Pitcher, T. J. (1986). *The behaviour of teleost fishes*. Croom Helm.

515 Popper, A. N. (1970). Auditory capacities of the Mexican blind cave fish (*Astyanax jordani*) and
516 its eyed ancestor (*Astyanax mexicanus*). *Animal Behaviour*, 18(PART 3), 552–562.
517 [https://doi.org/10.1016/0003-3472\(70\)90052-7](https://doi.org/10.1016/0003-3472(70)90052-7)

518 Raizen, D. M., Zimmerman, J. E., Maycock, M. H., Ta, U. D., You, Y., Sundaram, M. V., &
519 Pack, A. I. (2008). Lethargus is a *Caenorhabditis elegans* sleep-like state. *Nature*, 451, 569.
520 Retrieved from <https://doi.org/10.1038/nature06535>

521 Roberts, A. C., Reichl, J., Song, M. Y., Dearinger, A. D., Moridzadeh, N., Lu, E. D., ...
522 Glanzman, D. L. (2011). Habituation of the C-start response in larval zebrafish exhibits
523 several distinct phases and sensitivity to NMDA receptor Blockade. *PLoS ONE*, 6(12).
524 <https://doi.org/10.1371/journal.pone.0029132>

525 Saint-Amant, L., & Drapeau, P. (1998). *Time Course of the Development of Motor Behaviors in*
526 *the Zebrafish Embryo*. *J Neurobiol* (Vol. 37).

527 Shimazaki, T., Tanimoto, M., Oda, Y., & Higashijima, S.-I. (2019). Behavioral Role of the
528 Reciprocal Inhibition between a Pair of Mauthner Cells during Fast Escapes in Zebrafish.
529 *The Journal of Neuroscience : The Official Journal of the Society for Neuroscience*, 39(7),
530 1182–1194. <https://doi.org/10.1523/JNEUROSCI.1964-18.2018>

531 Shiriagin, V., & Korsching, S. I. (2019). Massive Expansion of Bitter Taste Receptors in Blind
532 Cavefish, *Astyanax mexicanus*. *Chemical Senses*, 44(1), 23–32.
533 <https://doi.org/10.1093/chemse/bjy062>

534 Shiriagin, V., & Korsching, S. I. (2019). Massive Expansion of Bitter Taste Receptors in Blind
535 Cavefish, *Astyanax mexicanus*. *Chemical Senses*, 44(1), 23–32.
536 <https://doi.org/10.1093/chemse/bjy062>

537 Stahl, B. A., Jaggard, J. B., Chin, J. S. R., Kowalko, J. E., Keene, A. C., & Duboué, E. R. (2019).
538 Manipulation of gene function in Mexican cavefish. *Journal of Visualized Experiments*,
539 2019(146). <https://doi.org/10.3791/59093>

540 Stil, A., & Drapeau, P. (2016). Neuronal labeling patterns in the spinal cord of adult transgenic
541 Zebrafish. *Developmental Neurobiology*, 76(6), 642–660.
542 <https://doi.org/10.1002/dneu.22350>

543 Suzuki, T. N. (2018). Alarm calls evoke a visual search image of a predator in birds.
544 *Proceedings of the National Academy of Sciences of the United States of America*, 115(7),
545 1541–1545. <https://doi.org/10.1073/pnas.1718884115>

546 Tabor, K. M., Bergeron, S. A., Horstick, E. J., Jordan, D. C., Aho, V., Porkka-Heiskanen, T., ...
547 Burgess, H. A. (2014). Direct activation of the Mauthner cell by electric field pulses drives
548 ultrarapid escape responses. *Journal of Neurophysiology*, 112(4), 834–844.
549 <https://doi.org/10.1152/jn.00228.2014>

550 Takahashi, M., Inoue, M., Tanimoto, M., Kohashi, T., & Oda, Y. (2017). Short-term
551 desensitization of fast escape behavior associated with suppression of Mauthner cell activity
552 in larval zebrafish. *Neuroscience Research*, 121, 29–36.
553 <https://doi.org/10.1016/j.neures.2017.03.008>

554 Temizer, I., Donovan, J. C., Baier, H., & Semmelhack, J. L. (2015). A Visual Pathway for
555 Looming-Evoked Escape in Larval Zebrafish. *Current Biology : CB*, 25(14), 1823–1834.
556 <https://doi.org/10.1016/j.cub.2015.06.002>

557 Walker, J. A., Ghalambor, C. K., Griset, O. L., McKenney, D., & Reznick, D. N. (2005). Do
558 faster starts increase the probability of evading predators? *Functional Ecology*, 19(5), 808–
559 815. <https://doi.org/10.1111/j.1365-2435.2005.01033.x>

560 Walsh, J. J., Christoffel, D. J., Heifets, B. D., Ben-Dor, G. A., Selimbeyoglu, A., Hung, L. W.,
561 ... Malenka, R. C. (2018). 5-HT release in nucleus accumbens rescues social deficits in
562 mouse autism model. *Nature*. <https://doi.org/10.1038/s41586-018-0416-4>

563 Wöhl, S., & Schuster, S. (2007). The predictive start of hunting archer fish: a flexible and precise
564 motor pattern performed with the kinematics of an escape C-start. *The Journal of
565 Experimental Biology*, 210(Pt 2), 311–324. <https://doi.org/10.1242/jeb.02646>

566 Yasugi, M., & Hori, M. (2012). Lateralized behavior in the attacks of largemouth bass on
567 Rhinogobius gobies corresponding to their morphological antisymmetry. *Journal of
568 Experimental Biology*, 215(14), 2390–2398. <https://doi.org/10.1242/jeb.068155>

569 Yoshizawa, M., Goricki, S., Soares, D., & Jeffery, W. R. (2010). Evolution of a behavioral shift
570 mediated by superficial neuromasts helps cavefish find food in darkness. *Current Biology :
571 CB*, 20(18), 1631–1636. <https://doi.org/10.1016/j.cub.2010.07.017>

572 Yoshizawa, M., & Jeffery, W. R. (2008). Shadow response in the blind cavefish *Astyanax*
573 reveals conservation of a functional pineal eye. *Journal of Experimental Biology*, 211(3),
574 292–299. <https://doi.org/10.1242/jeb.012864>

575 Yoshizawa, M., Yamamoto, Y., O’Quin, K. E., & Jeffery, W. R. (2012). Evolution of an
576 adaptive behavior and its sensory receptors promotes eye regression in blind cavefish. *BMC*
577 *Biology*, 10. <https://doi.org/10.1186/1741-7007-10-108>

578 Zeddies, D. G., & Fay, R. R. (2005). Development of the acoustically evoked behavioral
579 response in zebrafish to pure tones. *Journal of Experimental Biology*, 208(7), 1363–1372.
580 <https://doi.org/10.1242/jeb.01534>

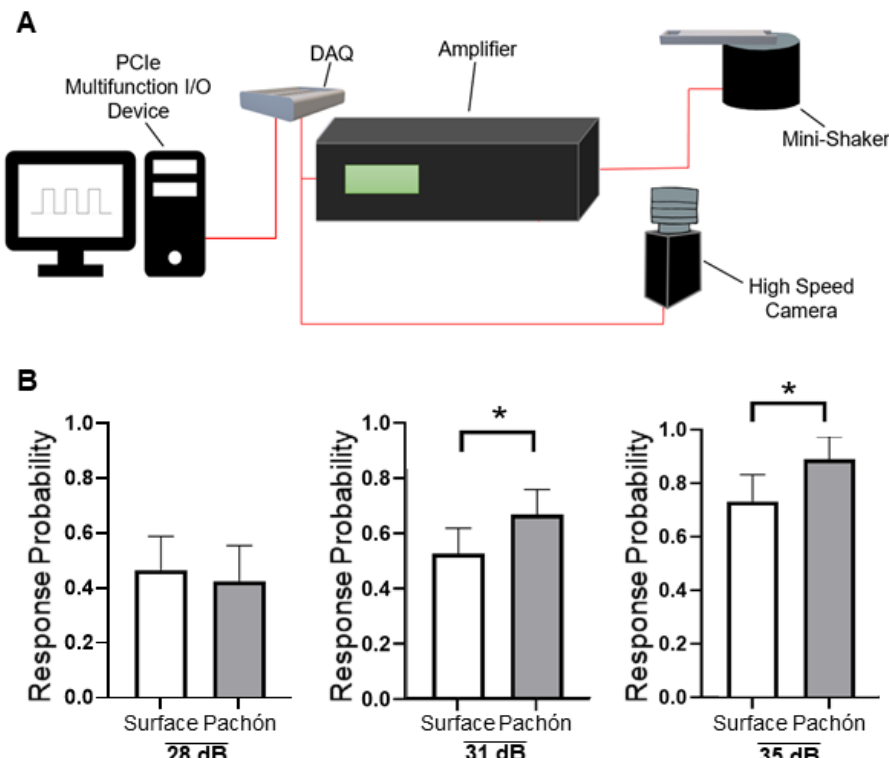
581 Zottoli, S. J., Kimmel, C. B., Metcalfe, W. K., Sagasti, A., Glanzman, D. L., & Papazian, D. M.
582 (2011). Correlation of the startle reflex and Mauthner cell auditory responses in
583 unrestrained goldfish. *Journal of Experimental Biology*, 66(1), 243–254.
584 <https://doi.org/858992>

585 Zottoli, S. J., Kimmel, C. B., Metcalfe, W. K., Sagasti, A., Glanzman, D. L., & Papazian, D. M.
586 (2011). Correlation of the startle reflex and Mauthner cell auditory responses in
587 unrestrained goldfish. *Journal of Experimental Biology*, 66(1), 243–254.
588 <https://doi.org/858992>

589

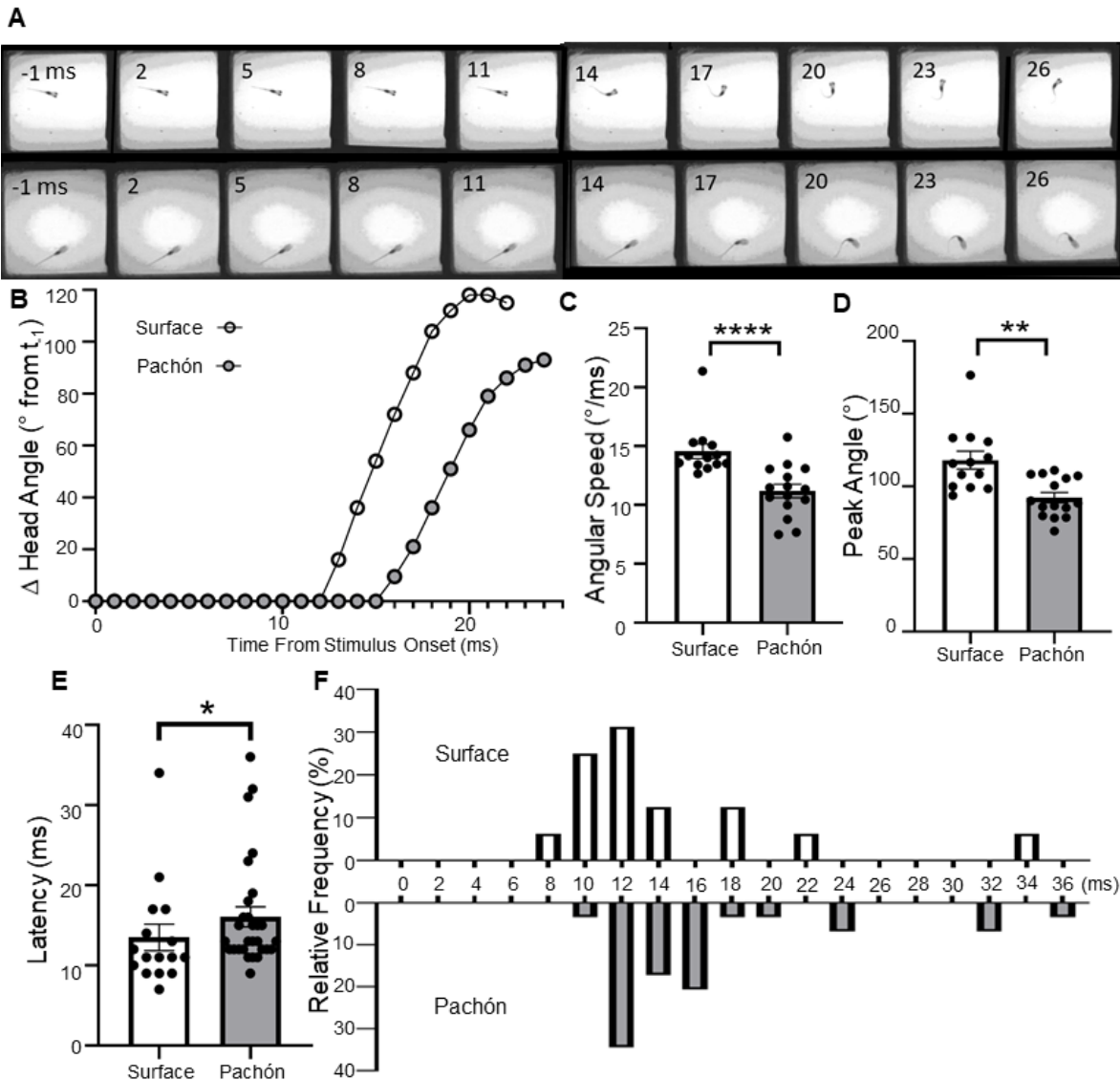
590 **Figure Legends**

591



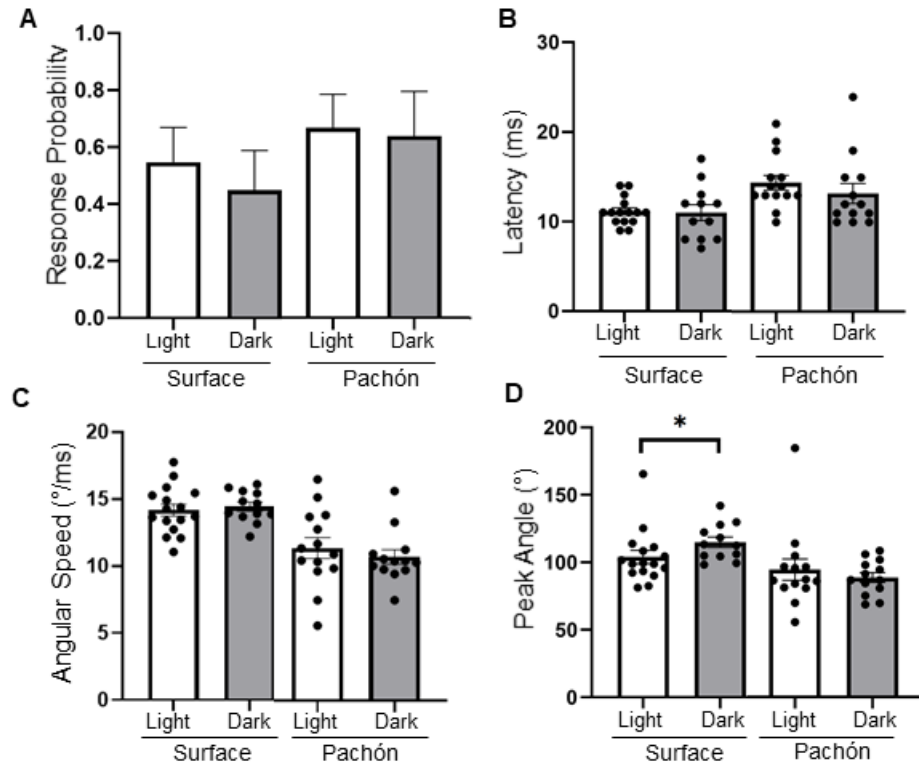
592

593 **Figure 1. Measurements of C-start response in *A. mexicanus*** (A) Acoustic stimuli
594 were generated using an amplifier and small vibration exciter controlled by a Data
595 acquisition device (DAQ). A high-speed camera collected data throughout the
596 stimulation protocol. (B) Pachón larvae (grey) exhibit increased startle probability to
597 vibrational stimuli at intensities of 31 dB (SF N=112, Pa N=103, 2-tailed Fisher's Exact
598 Test p=0.0374) and 35 dB (SF N=72, Pa N=48, 2-tailed Fisher's Exact Test p=0.0373)
599 compared to surface fish (white). No significant differences were detected at 28 dB (SF
600 N= 64, Pa N= 56, 2-tailed Fisher's Exact Test p=0.715). Error bars signify margin of
601 error. * denotes p≤0.05.

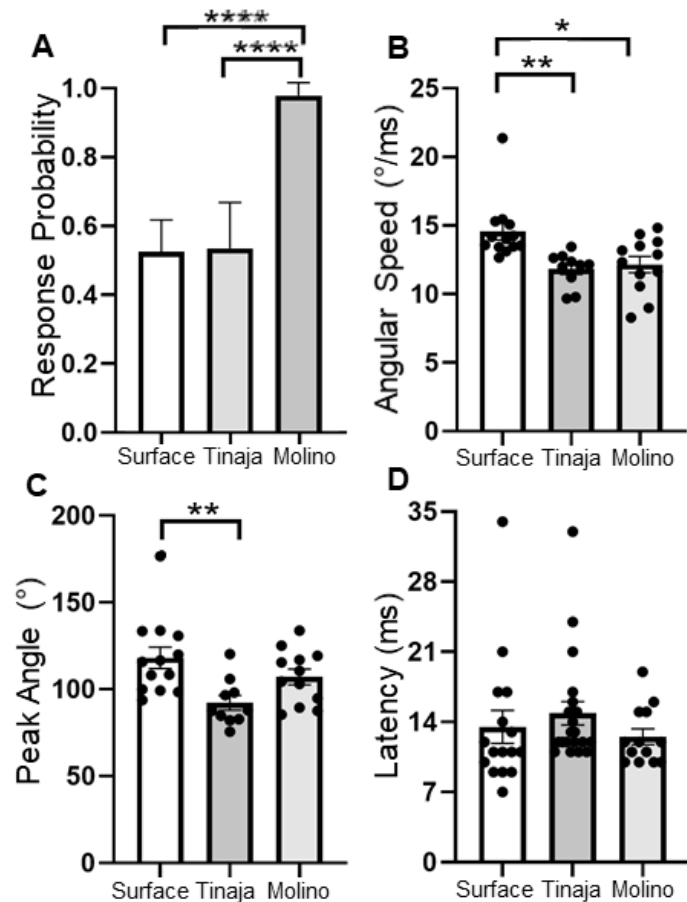


602

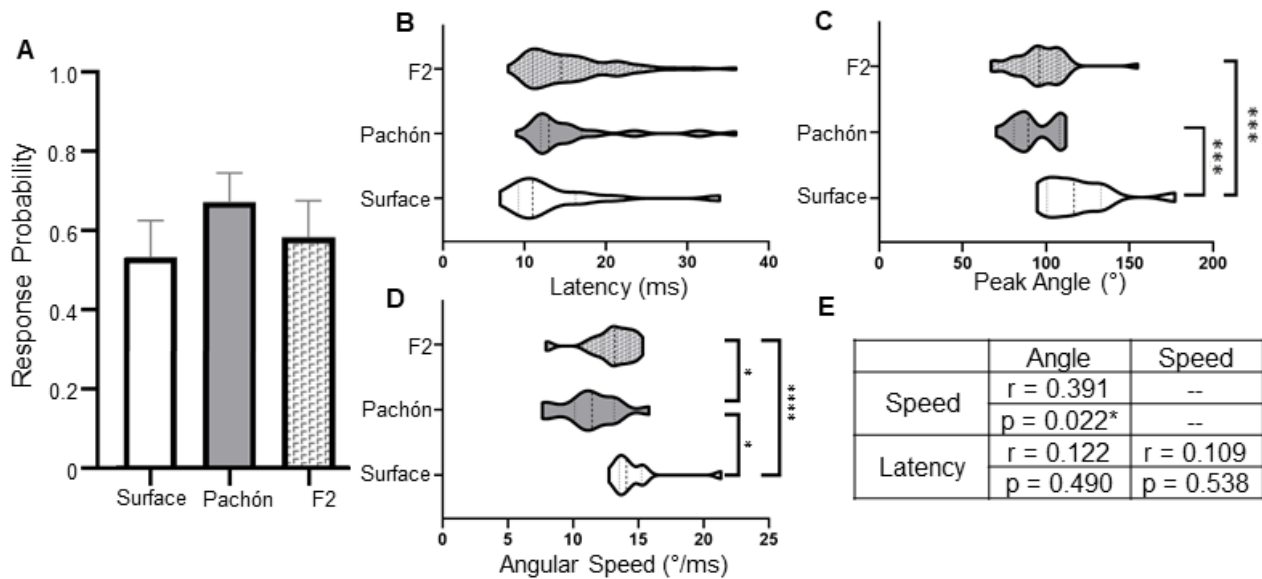
603 **Figure 2. C-start kinematics are altered in Pachón cavefish** (A) Time lapse images showing
604 typical surface fish (top) and Pachón cave fish (bottom) C-start responses. Changes in
605 orientation over the course of the response were standardized to the fish's orientation 1 ms
606 before stimulus onset (first frame shown). Snapshots shown are 3 ms apart (B) Surface fish
607 (open circles) and Pachón cavefish (filled circles) exhibit robust differences in c-start kinematics.
608 Quantitative analysis was done to compare the angular speed, peak bend angle, and latency of
609 surface and cave fish responses. (C) Comparisons of Pachón (N=15, median=11.34°/s) and
610 surface fish (N=13, median=14.01°/s) responses revealed that cavefish exhibit significantly
611 reduced turning speed than surface fish. Mann-Whitney U=17, $p<0.0001$. (D) Pachón cavefish
612 (N=15, median=88.36°) also exhibit a smaller change in orientation during the first phase of the
613 C-start response than surface fish (N=13, median 115.8°). Mann-Whitney U=29.50, $p=0.0011$.
614 (E) Initiation of Pachón responses (N=29, median=13ms) was delayed relative to surface fish
615 responses (N=16, median=11ms). Mann-Whitney U=145.5, $p=0.0386$. (F) A histogram of
616 response relative frequency across different response latencies reveals a shift in Pachón
617 cavefish (black) to slower response latency. Error bars denote std. error of mean. * denotes
618 $P\leq 0.05$. ** denotes $P\leq 0.01$, **** denotes $P\leq 0.0001$.



619
620
621 **Figure 3. Visual input influences escape trajectory of C-start responses in surface**
622 **fish** (A) The response probabilities of both surface fish (unfilled bars; light N=64, dark
623 N=49) and Pachón cavefish (filled bars; light N=60, dark=36) were unaffected by the
624 presence or absence of white light. Error bars signify margin of error. Surface fish:
625 Fisher's Exact test p = 0.345; Pachón: Fisher's Exact test p=0.827. (B) The Latency of
626 surface fish (light N=15, dark N=12) and Pachón cavefish (light N=14, dark N=13)
627 responses also were unaffected. Surface fish unpaired t-test t = 0.1467, df = 25, p =
628 0.8846; Pachón unpaired t-test t = 0.8779, df = 25, p = 0.8779. (C) Likewise, the angular
629 speed of surface fish (light N=16, dark N=12) and Pachón cavefish (light N=14, dark
630 N=13) were unaffected by light. (D) The peak bend angle of surface fish (light N=16,
631 dark N=12) was significantly larger in the absences of light. Median angle in light
632 conditions was 99.15° and 112.8° in the dark. 2-tailed Mann-Whitney test U = 46.50, p =
633 0.0204. Pachón cavefish exhibited no difference in peak bend angle in dark conditions.
634 Pachón 2-tailed Mann-Whitney test U = 87.50, p = 0.8774. * denotes p≤0.05. Error bars
635 on kinematic data (B-D) signify standard error of the mean.
636
637



638
639
640 **Figure 4. The C-start response is altered in Tinaja and Molino populations of**
641 **cavefish.** (A) Molino larvae (N=54) responded in 98% of trials, exhibiting significantly
642 higher response probability than either surface (N=112) or Tinaja (N=54) larvae. Error
643 bars denote margin of error. Surface/Molino $\chi^2(1)=32.28$, $p<0.0001$; Tinaja/Molino χ^2
644 (1)=26.292, $p<0.0001$. (B) There were no significant differences in response latency
645 (surface N=16, Tinaja N=21, Molino N=13). One-way ANOVA $F(2, 47) = 0.8153$,
646 $p=0.4487$. (C) Surface fish larvae (N=13) turned with significantly quicker angular speed
647 than Tinaja (N=10) or Molino (12) larvae. One-way ANOVA $F(2, 32)=0.7188$, $p=0.0024$.
648 Surface/Molino $p=0.0101$; surface/Tinaja $p=0.0051$. (D) Surface fish exhibited the most
649 drastic change in orientation. One-way ANOVA $F(2, 32)=0.7560$. Surface/Tinaja
650 $p=0.0044$. Error bars on kinematic data (B-D) denote standard error of the mean. *
651 denotes $p\leq 0.05$, ** denotes $p\leq 0.01$, **** denotes $p\leq 0.0001$.
652



653
654 **Figure 5. Analysis of surface-cave hybrids reveals a relationship between angular**
655 **speed and peak C-start angle (A)** No difference was identified between the response
656 probabilities of surface fish (N=112), Pachón (N=103), and F₂ hybrids (N=179), χ^2 (2,
657 N=291)=2.93, $p=0.099$, though surface and Pachón cavefish approached significance.
658 Error bars signify margin of error (B) There was also no difference in response latency
659 between surface (N=16), Pachón (N=29), and F₂ hybrids (N=68). (C) F₂ hybrids (N=34)
660 exhibit a peak change in orientation similar to that of Pachón (N=15) larvae, in contrast
661 to surface fish (N=13). One-way ANOVA $F(2, 59) = 0.66$, $p < 0.001$. Surface/Pachón
662 $p < 0.001$, surface/ F₂ $p < 0.001$. (D) The angular speed of the F₂ hybrids (N=34) was
663 intermediate to that of cavefish (N=15) and surface fish (N=13). One-way ANOVA $F(2,$
664 59) = 0.48, $p = 0.0002$. Surface/ F₂ $p=0.0426$, F₂/Pachón $p=0.0139$, surface/Pachón
665 $p < 0.0001$. (E) Spearman's rank correlation test indicates a positive correlation exists
666 between peak angle and speed. r denotes Spearman's correlation coefficient, rho.
667 Dotted lines in violin plots denote quartiles and median. * denotes $p \leq 0.05$, ** denotes
668 $p \leq 0.01$, *** $p \leq 0.001$.
669

670